Tech Science Press

Poly (Butylene Adipate-Co-Terephthalate) and Poly (Ɛ-Caprolactone) and Their Bionanocomposites with Cellulose Nanocrystals: Thermo-Mechanical Properties and Cell Viability Study

Marcia Cristina Branciforti[1,*], Caroline Faria Bellani[2], Carolina Lipparelli Morelli[2], Alice Ferrand[3], Nadia Benkirane-Jessel[3] and Rosario Elida Suman Bretas[2]

[1]Departamento de Engenharia de Materiais, Universidade de São Paulo, São Carlos, SP, Brasil.

[2]Departamento de Engenharia de Materiais, Universidade Federal de São Carlos, São Carlos, SP, Brasil.

[3]Institut National de la Santé et de la Recherche Médicale, Université de Strasbourg, Strasbourg, France.

[*]Corresponding Author: Marcia Cristina Branciforti. Email: marciacb@sc.usp.br.

Abstract: Although nanocomposites have recently attracted special interest in the tissue engineering area, due to their potential to reinforce scaffolds for hard tissues applications, a number of variables must be set prior to any clinical application. This manuscript addresses the evaluation of thermo-mechanical properties and of cell proliferation of cellulose nanocrystals (CNC), poly(butylene adipate-co-terephthalate) (PBAT), poly(ε-caprolactone) (PCL) films and their bionanocomposites with 2 wt% of CNC obtained by casting technique. Cellulose nanocrystals extracted from Balsa wood by acid hydrolysis were used as a reinforcing phase in PBAT and PCL matrix films. The films and pure CNC at different concentrations were cultured with osteoblasts MG-63 and the cell proliferation was assessed by AlamarBlue® assay. The thermal-mechanical properties of the films were evaluated by dynamic-mechanical thermal analysis (DMTA). It was found by DMTA that the CNC acted as reinforcing agent. The addition of CNCs in the PBAT and PCL matrices induced higher storage moduli due to the reinforcement effects of CNCs. The cell viability results showed that neat CNC favored osteoblast proliferation and both PBAT and PCL films incorporated with CNC were biocompatible and supported cell proliferation along time. The nature of the polymeric matrix or the presence of CNC practically did not affect the cell proliferation, confirming they have no *in vitro* toxicity. Such features make cellulose nanocrystals a suitable candidate for the reinforcement of biodegradable scaffolds for tissue engineering and biomedical applications.

Keywords: Cell viability; thermo-mechanical properties; cellulose nanocrystals (CNC); biocompatible polymers; tissue engineering; bionanocomposites

1 Introduction

The use of biodegradable and biocompatible polymers for the repair or replacement of diseased or damaged tissues has attracted interest in the tissue engineering area [1,2]. Biodegradable and biocompatible polymers play an important role in the formation of functional new tissues from transplanted cells and provide temporary scaffolding that guides the growth and organization of new tissues that is structurally integrated with the body [3].

A device must have adequate design and strength to be used as a biomaterial. The scarcity of polymers with appropriate characteristics for such application has motivated the search for novel biocompatible materials of improved mechanical properties [4]. Poly(butylene adipate-co-terephthalate) - PBAT - is an aliphatic-co-aromatic biodegradable and flexible copolymer [5] whose elongation at break is higher than that of most biodegradable polyesters [6]. Although some studies have indicated PBAT is a biocompatible polymer [6,7], this polymer has been scarcely studied for medical devices [6]. The main limitations include its poor thermal and mechanical resistance and restricted access to certain applications, as bone implants [6]. Poly(ε-caprolactone)-PCL-is a biodegradable, biocompatible in biological applications, and aliphatic linear semicrystalline polyester known for its high malleability. PCL was

approved for clinical use as a biological device and suture in 1980 and is considered to be a suitable substance for tissue engineering [8].

Some properties of PBAT and PCL as mechanical and thermal resistances must be improved for their application as biomaterials. Nevertheless, such drawbacks could be overcome through the addition of nano-sized fillers, as shown in some studies [6,9-12]. Furthermore, the addition of fillers in the polymer matrix can usually significantly improve the structure by acting as reinforcing agents.

In recent years, researchers have expressed a growing interest in exploring numerous biomedical applications of nanomaterials aiming to improve the life quality of patients who suffer of debilitating bone fractures, for example [13]. Some nanomaterials are able to increase mechanical strength, bioactivity and resorbability of resulting biomaterials [6,14,15]. Efforts to increase the mechanical properties of biodegradable polymers by the addition of cellulose nanocrystals (CNC) have been reported [12,16-19]. CNCs are obtained from cellulose, which is an abundant and not expensive biosource [8], biodegradable [20,21], with excellent mechanical properties, Young's modulus between 130 and 250 GPa, what makes them suitable candidates for polymer reinforcement [8,11,12,20,21]. CNCs can be produced from a variety of cellulose sources, including wood, cotton, natural fibers, tunicate, fungi or bacteria [8]. Although the commercial exploitation of CNC in various applications has already started, their toxic potential is little known and seems to be influenced by several factors [22,23]. Regarding the biomaterials, the toxic potential of CNC in terms of cytotoxicity must be known to ensure the biocompatibility and applicability of the final material in the tissue engineering area.

In this study, CNC obtained from Balsa wood [24] were incorporated in PBAT and PCL matrices through a solvent casting process. The resulting bionanocomposites were developed to overcome the polymers low mechanical strength and make them potentially interesting materials for biomedical applications, as tissue engineering. Recent studies conducted by our research group have demonstrated that the elastic modulus and tensile strength of PBAT increased with the addition of unmodified CNC for various compositions. Such results have confirmed composites with good CNC dispersion and distribution and good interfacial interaction between the CNC and the PBAT can be obtained by a casting process [11] or melt extrusion [12]. A biomaterial must have biocompatible surfaces to be used in tissue regeneration. However, biocompatibility assays related to cellulose nanocrystals and bionanocomposites of PBAT and PCL with CNC have not been widely reported in the literature. In this work, we evaluated the thermo-mechanical properties and cell proliferation/viability of pure CNC, PBAT, PCL, and their bionanocomposites (PBAT and PCL incorporated with CNC), prior to their production as scaffolds for applications in tissue engineering. The objective was to verify possible differences in rates of cell growth and/or cell viability caused by the CNC and resulting nanocomposites in comparison to pure PBAT and pure PCL. As these nanocomposites with improved mechanical strength are particularly interesting for further applications in bone tissue engineering, the cell proliferation was tested with osteoblast-like MG-63 cells, which have been extensively described in other studies [25-26].

2 Experimental Part

2.1 Materials

PBAT F BX7011 Ecoflex® was supplied by BASF and it has a weight-average molecular weight (Mw) of 140,000 g/mol and melting temperature of 110-120°C. PCL was purchased from Sigma-Aldrich with Mw of 60,000 g/mol and melting temperature of 60°C. CellCrown™ insert was supplied by Scaffdex®, Finland. Dulbecco's Modified Eagle Medium (DMEM) was purchased from GIBCO®, Invitrogen™. AlamarBlue® staining was acquired from Life Technologies™. The other chemical reagents were purchased from Synth.

2.2 Preparation of Cellulose Nanocrystals

CNCs were extracted from Balsa wood [24] following the procedure described by Morelli et al. [27].

The Balsa powder was treated four times with 2 wt% of sodium hydroxide aqueous solution, at 90°C, for 3 h, under mechanical stirring. This procedure was done in order to purify the cellulose pulp by removing others components like lignin and hemicellulose. Then the bleaching treatment was performed for 3 h at 90°C in solution containing equal parts of an acetate buffer solution and an aqueous sodium chloride solution (1.7 wt%). The bleaching was repeated twice. Subsequent bleaching further purifies the fibers leaving mostly cellulose only while hemicellulose and lignin are removed. The acid hydrolysis for the extraction of cellulose nanocrystals was performed in aqueous solution of sulfuric acid (65 wt%) for 75 min at 50°C. The suspension was then repeatedly centrifuged at 3500 rpm for 10 min in a Heraeus Megafuge 2.0 centrifuge. The supernatant was discarded until it became cloudy, which indicated the presence of CNC. The suspension was then subjected to dialysis with water until neutrality. Dried CNCs were obtained through freeze-drying for characterization.

2.3 Characterization of Cellulose Nanocrystals

The morphology of the cellulose nanocrystals was observed under a Philips CM 120 transmission electron microscope (TEM) with 120 kV acceleration voltage. A drop of an aqueous suspension with 0.01 wt% of cellulose nanocrystals was deposited on a carbon-coated grid, dried and stained with a uranyl acetate solution (2 wt%). The dimensions of approximately 100 cellulose nanocrystals were measured by Image-Pro Plus 4.5 software.

2.4 Preparation of Polymeric Films

The two polymers studied (PBAT and PCL) were solubilized (10 wt% polymer concentration in the final solution) in chloroform by magnetic stirring at room temperature for 2 h. Separately, the desired amount of cellulose nanocrystals were dispersed in chloroform by 60 min sonication, using an ultrasonic bath USC 1450 by Ultrasonic Cleaner. The polymer solution and cellulose nanocrystals suspension were mixed and solid films were obtained through casting of the final solution on glass plates followed by chloroform evaporation at room temperature. Films of pure PBAT, pure PCL and their nanocomposites with 2 wt% of cellulose nanocrystals (PBAT + 2 wt% CNC and PCL + 2 wt% CNC samples, respectively) were prepared.

2.5 Dynamic-Mechanical Thermal Analysis (DMTA)

DMTA was done in a DMA8000 equipment (PerkinElmer) using samples with dimension of 20 mm of length, 5 mm of width and thickness of 0.2 mm in the tension mode. For each composition, at least two samples were analyzed. The analyses were carried out between -70°C and 100°C to the PBAT samples and between -70°C and 60°C to the PCL samples with a heating rate of 3 °C/min, and a strain of 0.05%, that is, within the linear viscoelastic range. The damping coefficient (Tan δ), the storage modulus (E´), and the loss modulus (E´´) as a function of temperature were thus obtained.

2.6 Cell Culture, Proliferation, and Cytotoxicity Assessment

Osteoblast-like MG-63 cells were maintained in a DMEM medium supplemented with 10 % (v/v) fetal bovine serum (FBS), 1 % (v/v) penicillin and 1 % (v/v) streptomycin (100 mg/mL) under 37°C and atmosphere supplemented with 5% CO_2. For cell proliferation assay, the cells were trypsinized, counted and seeded at 1×10^4 per well on films samples. The culture medium was exchanged every two days, in order to maintain log phase of growth.

AlamarBlue® staining quantitatively measured the proliferation of cells on several human and animal lines, bacteria or fungi. Continuous cell growth maintains a reduced environment (fluorescent, red), whereas the inhibition of cell growth maintains an oxidized environment (non-fluorescent, blue) [28].

Samples of polymeric films (pure PBAT, pure PCL and their nanocomposites with CNC) were cut by an

18 mm round cutter. Each side of the samples was sterilized by ultraviolet (UV) radiation using wavelength of 254 nm, 30 W, for 20 minutes and with a distance from the source of 20 cm. The UV sterilization process was carried out in the mildest recommended conditions, in order to avoid possible degradation of the samples. The samples were then fixed between a sterile two-piece CellCrown™ insert for a 24-well tissue culture polystyrene (TCPS) plaque. Before cell seeding a final disinfection was performed by leaving overnight the TCPS plaques filled with ethanol (70%) and rinsing twice the wells with a phosphate buffered saline (PBS) solution. CNCs were sterilized by UV radiation for 40 minutes for the testing of their proliferation and diluted in fresh, sterile DMEM at 100 µg/ml by mechanical stirring. Dilutions of 50, 25, 12.5 and 6.25 µg/ml of CNC in DMEM were prepared by the addition of a cell culture medium. During the tests, the medium was replaced by a fresh one containing CNC, according to the tested concentration.

The cell proliferation was tested at 3, 7, 14 and 21 days after the cell seeding. AlamarBlue® was dissolved in a 10% (v/v) culture medium and applied to each well containing samples and two empty wells (control of AlamarBlue®). The cells were incubated at 37°C for 4 h. Absorbance was then measured at 570 nm and 600 nm wavelength, on a Multiskan Ex Primary EIA V 2.2 UV/VIS spectrophotometer.

Statistical analyses were performed by two-way ANOVA with GraphPad Prism® software (GraphPad, San Diego, CA, USA), using Bonferroni multiple comparisons test. Probability values $P < 0.05$ were considered statistically significant and the number of determinations was n = 4.

3 Results and Discussion

3.1 Characterization of Cellulose Nanocrystals

Transmission electron microscopy (TEM) proved the acid hydrolysis was successful in obtaining cellulose on a nanometric scale, as shown in Fig. 1. Dimension measurements showed average length (L) of 176 ± 68 nm and diameter (D) of 7.5 ± 2.9 nm of the cellulose nanocrystals (CNC), which resulted in a 25 aspect ratio (L/D). The CNC characterization by wide-angle X-ray diffraction and thermogravimetric analysis from previous study [27] showed CNC had cellulose I crystal structure, crystallinity of about 62% and onset temperature of thermal degradation of 226°C, which enable the use CNC as reinforcing filler for thermoplastics even in molding processes with polymer melts.
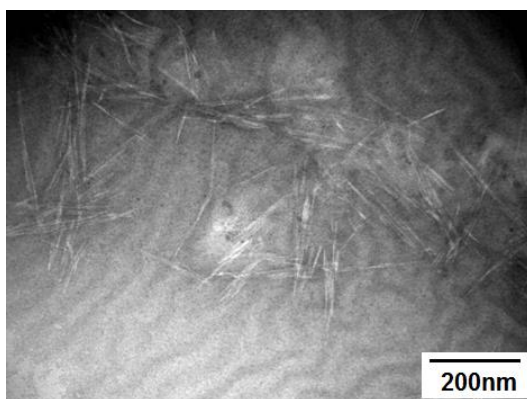

Figure 1: TEM micrograph of the CNC obtained from balsa wood

3.1 Characterization of films

3.1.1 Dynamic-Mechanical Thermal Analysis (DMTA)

Fig. 2(a) shows the dynamic-mechanical thermal analysis of the pure PBAT and PBAT + 2 wt% CNC nanocomposite as a function of temperature. The glass transition temperature (Tg) occurs where large segments of the chain start moving. DTMA data provides the relaxations temperatures and the transition peak of the Tan δ curve can be associated with the Tg of the polymer. The pure PBAT shows

two relaxation temperatures given by the peaks of Tan δ curve; the first one at -25.8 ± 0.7°C can be attributed to the movement of the butylene adipate units, whereas the second one at 42.5 ± 0.9°C can be attributed to the movement of the butylene terephthalate units. The Tg values of pure PBAT are in accordance with the literature [12,29]. The addition of CNC increased the first and the second relaxation temperatures of PBAT and reduced the relaxation peak heights. In the case of the first relaxation the temperature clearly increased from -25.8 ± 0.7°C to -20.9 ± 0.8°C. Such results indicate the decrease of freedom of movement of the polymer chains due the presence of CNC which acts as reinforcing filler. The storage modulus (E′) of PBAT was improved after the addition of CNCs. At room temperature, the addition of 2 wt% CNC increased by approximately 95% the PBAT storage modulus.

The same trend was observed for the DMTA results of the pure PCL and PCL + 2 wt% CNC nanocomposite, as shown in Fig. 2(b). The storage tensile modulus (E′) curve of pure PCL shows a main relaxation around -60°C associated with the glass transition and the irreversible polymeric chain flow around 50°C due to the melting of the PCL matrix. The Tan δ curves shown the relaxation temperature of PCL + 2 wt% CNC nanocomposite was about 4°C higher than that of the pure PCL, indicating the loss of mobility of the PCL chains due to the presence of CNC. The addition of 2 wt% CNC to the PCL increased its storage modulus at all temperatures; at room temperature, this increase was approximately 40%. The increase in glass transition temperature and the storage modulus improvement of PCL after the addition of CNC is due to the rigidity provided by the CNC which act as reinforcing filler and reduce PCL molecular chain mobility. Similar results have been reported by Zoppe et al. [20] and Siqueira et al. [30].
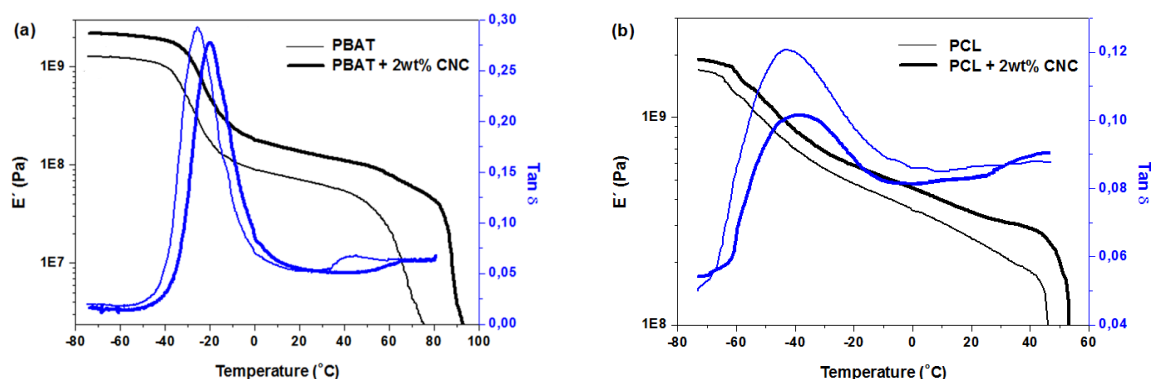

Figure 2: Storage modulus (E′) and Tan δ as a function of temperature of (a) PBAT and PBAT + 2 wt% CNC nanocomposite; (b) PCL and PCL + 2 wt% CNC nanocomposite films

3.1.2 Cell Proliferation

The cell proliferation study of pure CNC, PBAT, PCL, and their nanocomposites is crucial for their application as biomedical materials. AlamarBlue® staining proved a sensitive marker of cell viability, as the fluorescent/colorimetric product of mitochondrial activity is released outside only and by the viable cells into the medium, where it could be easily quantified by absorbance measurements.

Fig. 3 shows osteoblasts MG-63 proliferation rates measured by AlamarBlue® after 3, 7, 14 and 21 days for cells in direct contact with cellulose nanocrystals at various concentrations (6.25-100 µg/ml). For the initial phase (3 days), the same AlamarBlue® reduction (cell proliferation) for all samples was observed. At 7 days after the cell seeding, the results show the higher the CNC concentration, the bigger the cell proliferation rate and significant differences between the control and 12.5, 25, 50 and 100 µg/ml CNC concentrations were observed. Samples with 100 µg/ml of CNC reached almost 100% of AlamarBlue® reduction. After 14 days no significant cell proliferation was detected for 100 µg/ml CNC concentration in comparison with 7 days. A significant increase of cell proliferation for all other CNC

concentrations (from 6.25 to 50 µg/ml), though the cells cultivated with 25 and 50 µg/ml of CNC reached the maximum proliferation value (about 100%) with 14 days. 21 days after the cell seeding, all samples had reached an equitable cell proliferation, except for 100 µg/ml CNC samples, which showed a significant decrease in comparison to the control. According to Alberts et al. [31], when cell lines reach their maximum possible proliferation in a given space (i.e., the well of TCPS culture plate), the cell proliferation ceases almost entirely. As osteoblasts cultivated with 100 µg/ml reached the maximum cell proliferation first, the same also follows the decreasing of cell number first.

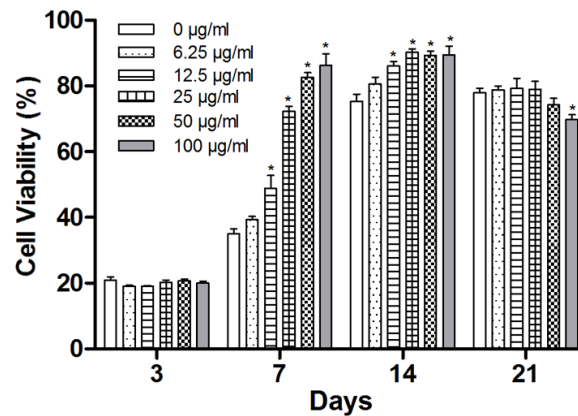**Figure 3:** Cell proliferation of CNC at different concentrations (µg/ml) measured by AlamarBlue® at 3, 7, 14 and 21 days. Each column represents the mean ± S.E.M. (Standard Error of the Mean) for n = 4. *$p < 0.05$

Overall, the higher the CNC concentration, the faster the cells maximum proliferation is. Due to their high polarity [8], neat CNCs seem to contribute to cell adhesion, hence, cell proliferation [32]. Moreover, as the cell proliferation assay was performed by direct contact, CNC lay down at the well bottom and altered the surface. According to Stevens et al. [33], nanoscale surface roughness greatly minimizes repulsive interactions and promotes adhesion. Surface effects are also greatly altered and the presence of nanoscale features increases cell attachment and proliferation [32,33]. Therefore, CNC contributes to cell proliferation due to its surface effect.

Fig. 4 shows the values of cell viability of osteoblasts cultivated in PBAT, PCL, and their nanocomposites films. For the sake of comparison, we presented the cell viability data from osteoblasts cultivated with 100 µg of CNC per ml of cell culture medium. MG-63 cells cultured on all films showed an increased cell proliferation rate throughout time, which indicates all films are biocompatible and support cell proliferation, as expected. Except at 3 days of assay, which there was a decrease for PCL samples, though follows a cell proliferation rate comparable with the others films. A remarkable cell proliferation rate can be observed for CNC alone in comparison with their composites, which can be explained by the surface and polarity effect of CNC [32,33], as previously elucidated.

Some statistical differences can be detected between the film samples, in the early days of cell culture (3 and 7 days), which were not continued. Because the cells were seeded in the log phase, the cells culture in this phase spread out and divided until each cell is attached to the dish and contacts its neighbors on all sides, until a confluent phase, while proliferation rates begins to fade [31]. Such a behavior can be explained by interactions of cells with one another and with the extracellular matrix, mediated by growth factors [31]. However, the biological activity and availability of the growth factor in a well depend not only upon its identity, but also upon how it is presented to the cells in space and over time [34,35]. In other words, as shown in Fig. 4, while the cell culture becomes confluent (from 14 days), the cell proliferation can be more due how these growth factors are present in log phase (which is not completely understood [31]) than the influence of substrate.
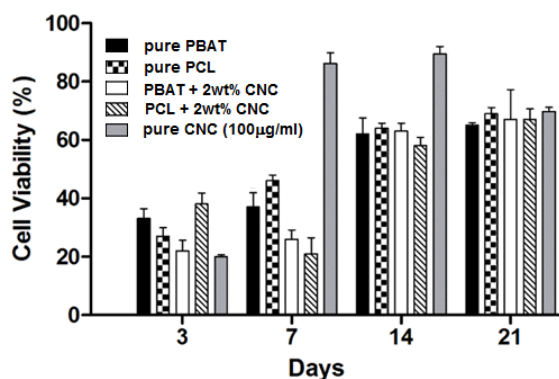
Figure 4: Comparison of cell proliferation of MG-63 on pure PBAT, pure PCL, PBAT + 2 wt% CNC and PCL + 2 wt% CNC nanocomposites films, and pure CNC (100 µg/ml, replicate of previous data) measured by AlamarBlue® assay at 3, 7, 14 and 21 days. Each column represents the mean ± S.E.M. (Standard Error of the Mean) for n = 4. $p < 0.05$

PBAT and PCL films with 2 wt% of CNC do not interfere with the osteoblasts proliferation/viability, in comparison with neat films, which emphasizes the non-cytotoxic character of CNC as previously reported for pure CNC. This is an essential requirement for a candidate material for potential applications in biomedical uses, as a reinforced material for uses in hard tissues like bone.

4 Conclusions

Cellulose nanocrystals were successfully extracted from Balsa wood and casting films of PBAT, PCL and their nanocomposites with 2 wt% of CNC were prepared. The thermo-mechanical properties and cell proliferation of pure CNC, PBAT, PCL, and their bionanocomposites were evaluated. It was found by DMTA that the CNC acted as reinforcing agent. The addition of CNCs in the PBAT and PCL matrices induced higher storage moduli due to the reinforcement effects of CNCs. Cell proliferation assay of pure CNC indicated CNC contributes to osteoblasts proliferation. The results of the cell proliferation analysis for PBAT and PCL films incorporated with CNC showed both support cell proliferation for MG63 cells. The nature of the polymeric matrix or the presence of CNC among the films practically does not affect the cell proliferation. Such features make cellulose nanocrystals a suitable candidate to reinforce those biodegradable polymers for biomedical applications.

References

1. Tian, H., Tang, Z., Zhuang, X. (2012). Biodegradable synthetic polymers: preparation, functionalization and biomedical application. *Progress in Polymer Science, 37,* 237-280.

2. Jang, J. H., Castano, O., Kim, H. W. (2009). Electrospun materials as potential platforms for bone tissue engineering. *Advanced Drug Delivery Reviews, 61,* 1065-1083.

3. Kim, B. S., Mooney, D. J. (1998). Development of biocompatible synthetic extracellular matrices for tissue engineering. *Trends in Biotechnology, 16,* 224-230.

4. Neff, J. A., Caldwell, K. D., Tresco, P. A. (1998). A novel method for surface modification to promote cell

attachment to hydrophobic substrates. *Journal of Biomedical Materials Research, 40,* 511-519.

5. Shi, X. Q., Ito, H., Kikutani, T. (2005). Characterization on mixed-crystal structure and properties of poly(butylene adipate-co-terephthalate) biodegradable fibers. *Polymer, 46,* 11442-11450.

6. Fukushima, K., Wu, M. H., Bocchini, S., Rasyida, A., Yang, M. C. (2012). PBAT based nanocomposites for medical and industrial applications. *Materials Science and Engineering: C, 32,* 1331-1351.

7. Goes, A. M., Carvalho, S., Oréfice, R. L., Avérous, L., Custódio, T. A. et al. (2012). Viabilidade celular de nanofibras de polímeros biodegradáveis e seus nanocompósitos com argila montmorilonita. *Polímeros, 22,* 34-41.

8. Eichhorn, S. J., Dufresne, A., Aranguren, M., Marcovich, N. E., Capadona, J. R. et al. (2010). Review: current international research into cellulose nanofibres and nanocomposites. *Journal of Materials Science, 45,* 1-33.

9. Bras, J., Hassan, M. L., Bruzesse, C., Hassan, C. A., El-Wakil, N. A. et al. (2010). Mechanical, barrier, and biodegradability properties of bagasse cellulose whiskers reinforced natural rubber nanocomposites. *Industrial Crops and Products, 32,* 627-633.

10. Siqueira, G., Bras, J., Follain, N., Belbekhouche, S., Marais, S. et al. (2013). Thermal and mechanical properties of bio-nanocomposites reinforced by Luffa cylindrica cellulose nanocrystals. *Carbohydrate Polymers, 91,* 711-717.

11. Morelli, C. L., Belgacem, M. N., Branciforti, M. C., Bretas, R. E. S., Crisci, A. et al. (2016). Supramolecular aromatic interactions to enhance biodegradable film properties through incorporation of functionalized cellulose nanocrystals. *Composites Part A: Applied Science and Manufacturing, 83,* 80-88.

12. Morelli, C. L., Belgacem, M. N., Branciforti, M. C., Salon, M. C. B., Bras, J. et al. (2016). Nanocomposites of PBAT and cellulose nanocrystals modified by in situ polymerization and melt extrusion. *Polymer Engineering & Science, 56,* 1339-1348.

13. Sahoo, S. K., Parveen, S., Panda, J. J. (2007). The present and future of nanotechnology in human health care. *Nanomedicine, 3,* 20-31.

14. Webster, T. J., Siegel, R. W., Bizios, R. (1999). Osteoblast adhesion on nanophase ceramics. *Biomaterials, 20,* 1221-1227.

15. Okamoto, M., John, B. (2013). Synthetic biopolymer nanocomposites for tissue engineering scaffolds. *Progress in Polymer Science, 38,* 1487-1503.

16. Bellani, C. F., Pollet, E., Hebraud, A., Pereira, F. V., Schlatter, G. et al. (2016). Morphological, thermal, and mechanical properties of poly(ε-caprolactone)/poly(ε-caprolactone)-grafted-cellulose nanocrystals mats produced by electrospinning. *Journal of Applied Polymer Science, 133,* 43445.

17. Luzi, F., Fortunati, E., Jiménez, A., Puglia, D., Pezzolla, D. et al. (2016). Production and characterization of PLA_PBS biodegradable blends reinforced with cellulose nanocrystals extracted from hemp fibres. *Industrial Crops and Products, 93,* 276-289.

18. Simão, J. A., Bellani, C. F., Branciforti, M. C. (2016). Thermal properties and crystallinity of PCL/PBSA/cellulose nanocrystals grafted with PCL chains. *Journal of Applied Polymer Science, 134,* 44493.

19. Borkotoky, S. S., Dhar, P., Katiyar, V. (2018). Biodegradable poly (lactic acid)/cellulose nanocrystals (CNCs) composite microcellular foam: effect of nanofillers on foam cellular morphology, thermal and wettability behavior. *International Journal of Biological Macromolecules, 106,* 433-446.

20. Zoppe, J. O., Peresin, M. S., Habibi, Y., Venditti, R. A., Rojas, O. J. (2009). Reinforcing poly(ε- caprolactone) nanofibers with cellulose nanocrystals. *Applied Materials & Interfaces, 1,* 1996-2004.

21. Maren, R., Shuping, D., Anjali, H., Yong, W. L. (2009). Cellulose nanocrystals for drug delivery. In: *Polysaccharide materials: performance by design*. American Chemical Society Publications.

22. Dong, S., Hirani, A. A., Colacino, K. R., Lee, Y. W., Roman, M. (2012). Cytotoxicity and cellular uptake of cellulose nanocrystals. *Nano Life, 2,* 1241006.

23. Lin, N., Dufresne, A. (2014). Nanocellulose in biomedicine: current status and future prospect. *European Polymer Journal, 59,* 302-325.

24. Branciforti, M. C., Marinelli, A. L., Kobayashi, M., Ambrosio, J. D., Monteiro, M. R. et al. (2009). Wood polymer composites technology supporting the recovery and protection of tropical forests: the Amazonian Phoenix Project. *Sustainability, 1,* 1431-1443.

25.   Pasqui, D., Torricelli, P., De Cagna, M., Fini, M., Barbucci, R. (2013). Carboxymethyl cellulose-hydroxyapatite hybrid hydrogel as a composite material for bone tissue engineering applications. *Journal of Biomedical Materials Research Part A, 102,* 1568-1579.

26.   Mattioli-Belmonte, M., Vozzi, G., Whulanza, Y., Seggiani, M., Fantauzzi, V. et al. (2012). Tuning polycaprolactone-carbon nanotube composites for bone tissue engineering scaffolds. *Materials Science and Engineering: C, 32,* 152-159.

27.   Morelli, C. L., Marconcini, J. M., Pereira, F. V., Bretas, R. E. S., Branciforti, M. C. (2012). Extraction and characterization of cellulose nanowhiskers from Balsa wood. *Macromolecular Symposia, 319,* 191-195.

28.   AlamarBlue® Technical Datasheet (2016). AbD Serotec Endeavor House, Langford Lane, Kidlington, Oxford, UK Corpright MorphoSys UK Ltd.

29.   Mohanty, S., Nayak, S. K. (2012). Biodegradable nanocomposites of poly(butylene adipate-co-terephthalate) (PBAT) and organically modified layered silicates. *Journal of Polymers and the Environment, 20,* 195-207.

30.   Siqueira, G., Bras, J., Dufresne, A. (2009). Cellulose whiskers versus microfibrils: influence of the nature of the nanoparticle and its surface functionalization on the thermal and mechanical properties of nanocomposites. *Biomacromolecules, 10,* 425-432.

31.   Alberts, B., Johnson, A., Lewis, J., Raff, M., Roberts, K. et al. (2002). Molecular biology of the cell, 4th ed. New York: Garland Science.

32.   Lampin, M., Warocquier-Clérout, R., Legris, C., Degrange, M., Sigot−Luizard, M. (1997). Correlation between substratum roughness and wettability, cell adhesion, and cell migration. *Journal of Biomedical Materials Research, 36,* 99-108.

33.   Stevens, M. M., George, J. H. (2005). Exploring and engineering the cell surface interface. *Science, 310,* 1135-1138.

34.   Hubbell, J. A. (1999). Bioactive biomaterials. *Current Opinion in Biotechnology, 10,* 123.

35.   Dinbergs, I. D., Brown, L., Edelman, E. R. (1996). Cellular response to transforming growth factor-beta1 and basic fibroblast growth factor depends on release kinetics and extracellular matrix interactions. *Journal of Biological Chemistry, 271,* 29822-29829.